2023 International Conference on Optical MEMS and Nanophotonics (OMN) and SBFoton International Optics and Photonics Conference (SBFoton IOPC) | 979-8-3503-0402-2/23/$31.00 ©2023 IEEE | DOI: 10.1109/OMN/SBFOTONIOPC58971.2023.10230917

Thermophoretic efficiency in the MCVD process: A CFD modeling

Rubens Cavalcante da Silva
University of São Paulo
São Paulo, Brazil
rubensrcs@usp.br
orcid.org/0000-0002-9794-0992

Paulo Jorge Duda de Morais
University of São Paulo
São Paulo, Brazil
orcid.org/0000-0002-4336-2963

Andre Carvalho
University of São Paulo
São Paulo, Brazil
orcid.org/0000-0001-8569-9532

Wagner de Rossi
Centro de Lasers e Aplicações IPEN-CNEN/SP
São Paulo, Brazil
orcid.org/0000-0003-1371-7521

Claudio Costa Motta
University of São Paulo
São Paulo, Brazil
orcid.org/0000-0002-2508-7320

***Abstract*—The thermophoretic efficiency in the modified chemical vapour deposition (MCVD) process has been numerically determined under specified conditions of temperature and velocity field in the silica deposition tube. A CFD code was used to solve a steady-state numerical model of the MCVD process. The cumulative efficiency of SiO_2 and GeO_2 deposition was calculated along the tube length, yielding to a maximum value of 42% and 37% respectivelly.**

***Index Terms*—MCVD, CFD, Thermophoretic Efficiency.**

I. Introduction

The modified chemical vapor deposition (MCVD) process is widely used for the manufacture of high quality optical fiber preforms. In this process, reactant species, e.g. $SiCl_4$, $GeCl_4$ and O_2 flow through a rotating silica tube and are heated by a moving exterior torch which traverses back and forth along the tube. Chemical reactions then take place and oxide particles are formed and deposit due to thermophoresis on the inner surface of the tube, although some particles flow out of the tube without depositing [1]. The correct determination of this deposition efficiency would allow a minimization of production cost, making the industrial process more advantageous. Fig. 1 shows a schematic representation of MCVD process and equations (1) and (2) represents the chemical reaction of formation of SiO_2 and GeO_2.

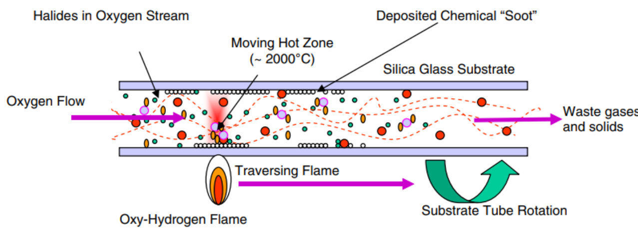

Fig. 1. Schematic representation of the MCVD process [2].

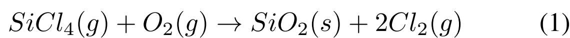

$$SiCl_4(g) + O_2(g) \rightarrow SiO_2(s) + 2Cl_2(g) \quad (1)$$

$$GeCl_4(g) + O_2(g) \leftrightarrow GeO_2(s) + 2Cl_2(g) \quad (2)$$

II. Theoretical Modeling

The theoretical modeling and boundary conditions of the simulations were based on [3], where the authors used the STAR-CCM+ CFD code to solve the coupled governing equations. The physical phenomenon considered in this study is the irreversible oxidation reactions of $SiCl_4$ and $GeCl_4$ carried by a oxygen flow inside a rotating tube, whose wall is heated by an external torch temperature profile. The flowrate at the inlet for each reactant is is 2 L/min for O_2, 3 mol/m^3 for $SiCl_4$ and 1.9 mol/m^3 for $GeCl_4$. During the MCVD process, the tempertaure of the gases at inlet is 300 K, the maximum torch temperature is 1800 K and the tube rotation rate is 45 rpm.

A. Mathematical and Computational Modeling

The three-dimensional steady-state numerical model established to determine the thermal flow field of MCVD process solves the continuity, momentum, energy and species equations, according to Eqs. (3) to (6) respectively, by means of the finite volume method.

$$\nabla . \left(\rho \vec{V}\right) = 0 \quad (3)$$

$$\rho \left(\vec{V} . \nabla\right) \vec{V} = -\nabla p + \mu \nabla^2 \vec{V} \quad (4)$$

$$\rho c_p \nabla T = \nabla . \left(\kappa \nabla T\right) + \Delta H r \quad (5)$$

$$\rho \vec{V} . \nabla Y_i = \nabla . \left(\rho D_i \nabla Y_i\right) - r \quad (6)$$

The efficiency formulation was based on [4] and considers the ratio between the flux of reactants and oxide particles along the tube. The particle flux at the tube inlet is given as:

Authorized licensed use limited to: UNIVERSIDADE DE SAO PAULO. Downloaded on November 14,2023 at 14:54:45 UTC from IEEE Xplore. Restrictions apply.

$$M = \rho u_0 \omega_0 \pi R^2 \tag{7}$$

where u_0 is the velocity and ω_0 is the mass fraction at the inlet.

The flux of deposition particles was determined to each nondimensional axial position ξ taking into account the radial component of the thermophoretic velocity. Hence, the mass flux of particle that reaches a wall surface of $2\pi R dx$ is:

$$dM = \begin{cases} 2\pi R \rho v_T(\xi, R)\omega(\xi, R)d\xi & \text{if } v_T > 0 \\ 0 & \text{if } v_T \leq 0 \end{cases} \tag{8}$$

where v_T is the radial component of the thermophoretic velocity defined as a function of the thermophoretic coefficient K, and the radial gradient of the temperature:

$$v_T = -\frac{K\nu}{T}\frac{\partial T}{\partial r} \tag{9}$$

Hence, the efficiency at the position ξ is defined as the rate of the particle flux incident in the wall (Eq. (8)) and the total particle flux in the tube (Eq. (7)):

$$E(\xi) = \frac{1}{\rho u_0 \omega_0 \pi R^2}\int_0^{\xi} dM \tag{10}$$

III. Numerical Results

The thermophoretic velocity field was determined by means of the temperature gradient along the computational domain. Fig. 2 shows the field of the radial component of thermophoretic velocity calculated by the Eq. (9). One can see that the maximum values of thermophoretic velocity are located near the wall and after the torch position, where the particle deposition tends to occur more intensively.

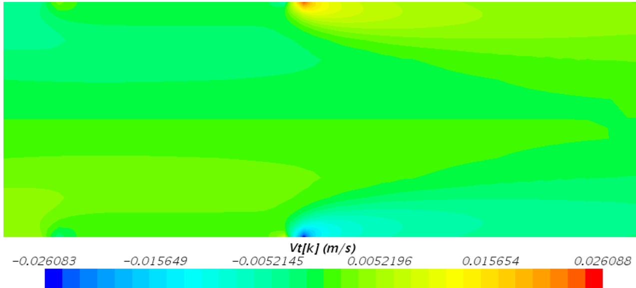

Fig. 2. Radial thermophoretic velocity field along the longitudinal section of the tube. The maximum values, located on the red (upper wall) and blue (lower wall) regions, are due to the highest temperature gradients.

The oxide concentration obtained as the solution of Eq. (6) is shown in Fig. 3. The oxide formation occurs predominantly near the wall due to the effect of the external torch heating. The deposition efficiency is presented in Fig. 4 in its cumulative form along the tube length for each case of oxide deposition. One can observe that the cumulative efficiency of GeO_2 presents lower values if compared to SiO_2. Moreover, the results are in accordance with the typical values presented other studies. For instance, the results of [5] varied between 30% to 50% depending on the flow regime (e.g. maximum torch temperature, reactant concentration).

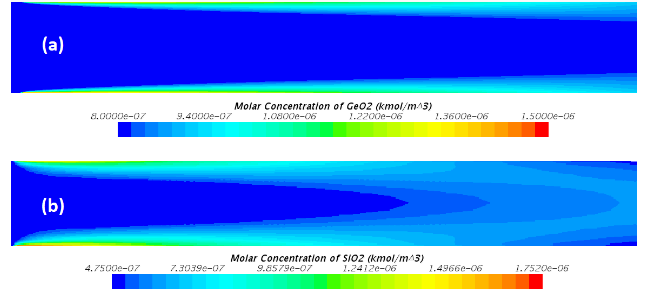

Fig. 3. (a) GeO_2 concentration and (b) SiO_2 concentration along the longitudinal section of the tube. The intense oxide formation occurs in the hottest region (near the wall) due to the torch heating

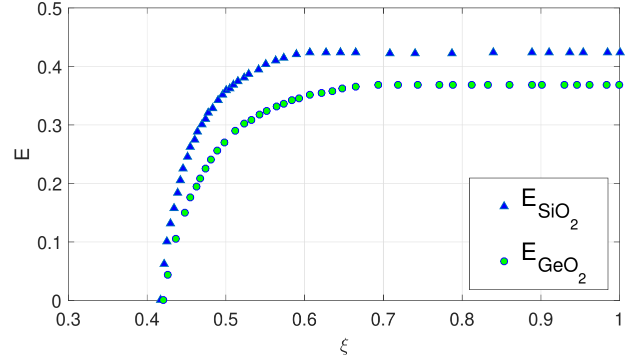

Fig. 4. Cumulative thermophoretic efficiency of SiO_2 and GeO_2 deposition along the tube length. The maximum value to each oxide is 42% and 37% respectivelly

IV. Concluding Remarks

A steady-state numerical analysis of heat transfer and fluid flow has been carried out for modified chemical vapor deposition (MCVD) process. The thermophoretic velocity and oxide concentration fields were determined and the thermophoretic efficiency of deposition of SiO_2 and GeO_2 was calculated by means of the species mass flux inside the tube domain. Further studies are being developed to improve the calculation of the deposition efficiency and consider the particle trajectories inside the domain.

References

[1] S. Joh, and R. Greif "The effects of $SiCl_4$ and $GeCl_4$ oxidation, variable properties, buoyancy and tube rotation on the modified chemical vapor deposition process"International Journal of Heat and Mass Transfer, vol. 34, 10, pp. 1911—1921, 1995.

[2] C. K. W. Cheung, D. Haley, D. F. Fletcher, G. W. Barton and P. McNamara "Simulation of particle–vortex interactions in the modified chemical vapor deposition process"Journal of Non-Crystalline Solids, 353, pp. 4066—4075, 2007.

[3] R. C. da Silva, P. J. D. de Morais, A. Carvalho, W. de Rossi and C. C. Motta "Numerical simulation on modified chemical vapor deposition (MCVD) thermal flow field"Proceedings of the IEE, 2022.

[4] M. F. Naccache "Estudo da deposição termoforética de partículas na fabricação de fibras óticas"Master Thesis (PUC-RJ), 1986.

[5] K. S. Park and M. Choi "Conjugate heat transfer and particle deposition in the modified chemical vapor deposition process: effects of torch speed and solid layer"International Journal of Heat and Mass Transfer, 1994.

Authorized licensed use limited to: UNIVERSIDADE DE SAO PAULO. Downloaded on November 14,2023 at 14:54:45 UTC from IEEE Xplore. Restrictions apply.